Polymer Bulletin 58, 465–478 (2007)
DOI 10.1007/s00289-006-0678-0

Polymer Bulletin

Phase morphology development of polypropylene/ethylene-octene copolymer blends: effects of blend composition and processing conditions

Xinhua Xu (✉), Xueliang Yan, Tianbing Zhu, Chunhuai Zhang, Jing Sheng

School of Materials Science & Engineering, Tianjin University, Tianjin 300072, China
E-mail: xhxu@tju.edu.cn, Fax: +86 22 27406127

Received: 4 May 2006 / Revised version: 19 July 2006 / Accepted: 24 August 2006
Published online: 12 September 2006 –

Summary

Blends of polypropylene (PP)/ethylene-octene copolymer (EOC) was studied. The influences of blend composition and processing conditions on phase morphology development of the blends were investigated by scanning electron microscopy (SEM) in detail. The minor composition formed the dispersed phase and the major composition formed the continuous phase, and the blends formed interpenetrating co-continuous morphology just at the intermediate concentration. The effect of concentration on phase coarsening was explained by the increase of dispersed phase coalescence with dispersed phase concentration's increase. Phase coarsening and phase fine dispersing were studied. The effect of mixing time on phase morphology development of the blends was investigated, the PP/EOC (80/20) blends has already formed a well-established droplet/matrix morphology after 1.5 min of mixing, and the similar blends phase morphology persisted until 11 min of mixing. The most prominent phenomenon is that the dispersed phase domain deformed from spherical droplet to elliptical droplet, even fibrillar or sheet morphology as the rotor speed increased. The increase of shear rate and elasticity ratio was applied to interpret this phenomenon.

Introduction

Polymer blends have received much attention in polymer science and industry field during the last 30 years. The research growth of polymer blends is mainly due to their ability to combine to the component properties in a blend product. The properties of polymer blends are a strong function of the blends morphology. The factors affecting the evolution of blends phase morphology during the melt blending include: (1) process parameters (mixing temperature, rotation speed of the rotor, mixing time, nature of the mixer type, quenching, annealing, etc.), (2) blend composition, (3) viscosity ratio, (4) interfacial tension, (5) elasticity ratio.

Polymer blends show two main morphology types: dispersed/matrix phase morphology and co-continuous morphology. Generally speaking, the forming of phase morphology is mainly due to the blend composition, the major component forms a continuous phase and the minor component forms a discrete phase [1-7], but in spite

of a component of having a higher content in the blends, one can't be certain that it will form the continuous phase, the viscosity ratio between dispersed phase and matrix phase influences the phase morphology too [8-11]. Besides, the main morphology is also dependent on the process parameters (mixing temperature, rotation speed of the rotor, mixing time) [12-26]. Process parameters (quenching, annealing, etc.) are also responsible for the morphology stability during further processing step [10,27]. The effects of viscosity ratio and interfacial tension on phase morphology are also very important. The classical studies based on Wu's investigation [28] and Favis BD's investigation [29] gives the relationship among the particle size, viscosity ratio, and interfacial tension. VanOene H [30] pointed out that in addition to the viscosity ratio and interfacial tension of the two liquids, the elasticity ratio also plays a crucial role in the deformability of drop.

PP is one of the most versatile commodity polymers because of its excellent properties. It has good chemical and moisture resistance, ductility, stiffness and low density. But its application is limited by its low impact resistance. In order to improve the low impact intensity, the blends of PP and thermoplastic elastomer are researched widely. Recently, Dow Elastomers Company produces a thermoplastic elastomer, EOC, which is a copolymer of ethylene and octene using metallocene technology. When EOC is added to PP, it provides enhanced impact properties for automotive exteriors and interiors and other applications requiring superior low temperature performance. Da silva ALN [31] compared this blends with EPDM modified polypropylenes and declared that a better processability was noted when EOC was used as an impact modifier. Due to the excellent performance, the blends of PP and EOC have attracted much attention.

Most of the existing investigation on PP/EOC blends has mainly focused on mechanical properties and rheological properties of low EOC content. For instance, Da silva ALN and his co-workers investigated comprehensively the rheological properties of PP/EOC blends [32,33], Paul S and Kale DD studied the rheological properties and mechanical properties of PP-cp/EOC blends [34,35]. Yang JH [36] studied the brittle-ductile transition of PP/EOC blends in both impact and high speed tensile tests. McNally T [37] investigated the influence of composition on rheology, mechanical properties and phase morphology in PP/EOC of 1-30 wt.% EOC. Kontopoulou M and his partners [38] compared the effect of composition on rheology, morphology, thermal and mechanical properties of PP/EOC and PP/ethylene-butene copolymer. In addition, Carriere CJ and Silvis HC [39] measured the interfacial tension between PP and polyolefin elastomer by using the imbedded fiber retraction technology and evaluated the effect of polyolefin elastomer type on the interfacial tension of PP/polyolefin elastomer blends. However, no detailed examination has been done on the morphology development of PP/EOC blends as a function of blend composition, process parameters until recently. The main objective of this article was to analyze quantitatively the influence of blend composition and processing conditions on phase morphology development of the PP/EOC blends.

Experimental

Materials

Polypropylene (PP1300) supplied by Yanshan Petrochemical Company, China, and EOC (Engage 8150, a metallocene catalysed copolymer of ethylene and 1-octene with

25 wt% of comonomer) provided by DuPont Dow Elastomers Company were used in this study. Characteristics of the polymers used are given in table 1.

Table 1. Characteristics of the polymers used in this work

Polymer	Density ($g \cdot cm^{-3}$)	MFI (g/10min)[a]
PP	0.90	1.1
EOC	0.868	0.5

[a] For PP, MFI was measured under 2.16 kg at 230°C. For EOC, MFI was measured under 2.16 kg at 190°C.

Rheological measurement

Discs of 25 mm in diameter and 1 mm in thickness were prepared by compression molding for PP and EOC under a pressure of 24.5 MPa at 180 °C for 10 min. The viscosity and modulus of PP and EOC were measured using a Stress Tech Fluid Rheometer (Model: Stress Tech, Relogical Instrument AB, Sweden), a parallel plate configuration was used with a gap of 1.0 mm and plate diameter of 25 mm. Shear rate sweep was performed, and the shear rate range used was 0.01-10 s^{-1} at 180 °C, the storage modulus was determined at 180 °C over a frequency of 0.01-100 Hz. A capillary rheometer (Model: XLY-2, Jilin University Science Education Company, China) with a capillary diameter of 1.0 mm and a length-to-diameter ratio of 40 was used to measure the viscosities of the samples at high shear rates ranging from 10 to 500s^{-1} at 180 °C. The Bagley and Rabowitsh correction were not made.

Blend preparation

PP and EOC were mixed in a rubber mixer (Model: XSM-1/20-80). The morphology development of the blends was studied as a function of blend ratio, mixing time, rotor speed. Blends with different compositions [PP/EOC=10/90, 20/80, 30/70, 40/60, 50/50, 60/40, 70/30, 80/20, 90/10, by weight] were prepared at a rotor speed of 40 rpm for 10 min at 180 °C. In order to study the effect of mixing time on phase morphology evolution, the blend experiments were performed at constant rotor speed of 50 rpm at 180 °C. The mixing time was varied from 1, 1.5, 2, 3, 4, 5, 7, 11min. The effect of shear rate on phase morphology development was investigated by varying the rotor speed.

Morphological characterization

The samples were fractured under liquid nitrogen for at least 10 min to make sure that the fracture is sufficiently brittle and one of the phases was preferentially extracted. Because it is difficult to extract the PP phase without affecting the EOC phase by using the solvent, all samples were etched in heptane at 60 °C to extract the EOC phase. In order to retain phase morphology, the etching time for different compositions is decided by repeated experiments. All samples were dried for 72 hours and coated with gold prior to SEM examination, an XL30ESE scanning electron microscopy operating at 25 KV was used to observe the specimens, several microscopy photographs were taken for each sample.

The photographs were quantitatively analyzed using the IMAGE PRO software. The drop diameter was calculated after analysis of the SEM microscopy photographs.

About 200-500 particles were considered to calculate the results. The diameter of a particle was defined by its average length of diameter that was measured at 2 degree intervals passing through the droplet's centroid. The number average diameter (D_n) and the volume average diameter (D_v) are defined by:

$$D_n = \frac{\sum_i n_i D_i}{\sum_i n_i} \quad (\mathbf{1})$$

$$D_v = \frac{\sum_i n_i D_i^4}{\sum_i n_i D_i^3} \quad (\mathbf{2})$$

Where D_i is the diameter of each droplet and n_i is the number of droplet with a diameter D_i.

Results and Discussion

The rheological properties of pure PP and pure EOC

The viscosity (η) versus shear rate (γ) plot for pure PP and pure EOC at 180 °C is shown in Fig. 1. It is evident from the curve that the viscosity of the pure polymer decreases with the increase of shear rate, indicating the pseudoplastic nature of the polymer. The viscosity of PP over the shear rate range investigated is greater than EOC. The shear thinning behavior of PP is more noticeable than EOC at lower shear rates, while an inverse behavior is observed at high shear rates. Fig. 2 gives the relationship between storage modulus (G') and frequency (ω) for pure PP and pure EOC at 180 °C. The storage modulus increases with increasing frequency. It is evident that the storage modulus of PP over the frequency range investigated is higher than EOC, while the storage modulus of EOC increases faster than PP. The storage modulus represents the elasticity of a material. So the elasticity ratio between EOC and PP increases progressively with the increase of frequency.

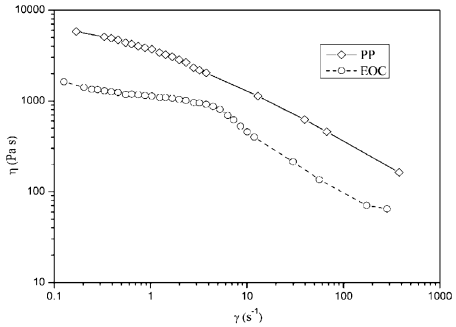

Fig. 1. The viscosity (η) as a function of shear rate (γ) for pure PP and pure EOC at 180 °C.

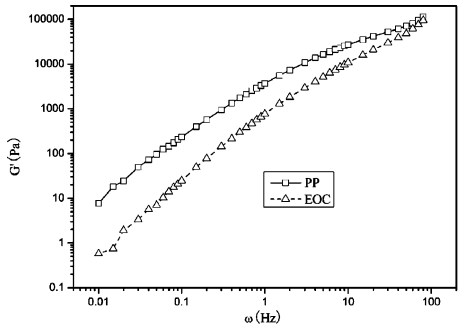

Fig. 2. The storage modulus (G') as a function of frequency (ω) for pure PP and pure EOC at 180 °C.

Paul S and Kale DD [33] checked the validity of the Cox–Merz rule in the PP-cp/EOC blends, pure PP-cp and EOC, accordingly, $\eta^*(\omega) = \eta(\gamma)$, and found that the two viscosities matched each other at equal values of shear rates or frequencies. So it is reasonable to consider that the frequency is consistent with shear rate in our study.
In the mixer, the materials were subjected to the complex shear and elongational deformation, and the complex temperature field. It is very difficult to determine the shear rate matching the speed of rotation exactly. So a simplified formula is used to relate the shear rate to the rotor speed, which based on Li JS's research in our lab [40]:

$$\gamma\left(s^{-1}\right) = 1.6 \times V_a\left(rpm\right) \quad (\mathbf{3})$$

Where γ is the shear rate and V_a represents the rotor speed. We are well aware of the fact that the formula adopted here is not rigorous, but we have done this only to relate the rotor speed to shear rate, thus enabling us to estimate the viscosity ratio and elasticity ratio of the constituent components. The viscosity ratio (p) and elasticity ratio of different rotor speeds of pure PP and pure EOC are given in table 2.

The effect of blend composition on the phase morphology development of PP/EOC blends

A lot of studies have been made about the effect of blend composition on phase morphology in polymer blending. Different polymer pairs have been intensively investigated recently [1-11]. The influence of the blend ratio on the phase morphology of the polystyrene (PS)/nylon 6 blends in whole range composition was analyzed by Nair SV and his partners [1]. Similar results were observed by Thomas S in Nylon 6/ EPDM blends [10] and Joseph S in PS/PB blends [3].
In Fig. 3, the morphology of PP/EOC blends with different compositions at 180 °C is depicted, which were prepared at the rotor speed of 40 rpm for 10 min. The light area of the SEM photomicrographs represents the PP phase and black for the EOC phase. The number average diameter (D_n) and the volume average diameter (D_v) of the dispersed phase droplets as a function of the PP concentration are given in Fig. 4. The D_n and D_v are defined by Eq. (1) and Eq. (2), respectively.
In the photomicrograph of phase morphology which is based on 10 wt.% PP concentration (Fig. 3(a)), no very evident spherical protuberance is found. That is likely because of the fact when the blends with fine-dispersed PP phase were etched by heptane to remove the EOC component, some fine-dispersed PP droplets may be eliminated simultaneously due to its subtle volume. The D_n and D_v of dispersed phase droplets are 0.2 μm and 0.66 μm, respectively (Fig. 4). The PP domain size ranged from 0.2 to 0.6 μm in diameter (Fig. 5). The photomicrographs which are based on 20 wt.%, 30 wt.% PP concentration show that the PP phase is preferentially dispersed as spherical protuberance in the low viscosity EOC matrix (Fig. 3(b),(c)). The D_n and D_v of 20 wt.% and 30 wt.% PP concentration are given in Fig. 4. With the increase of the PP content of the blends to 40wt% (Fig 3(d)), it can be seen that the structure and shape of the particles were very complex and PP became partially continuous with the coexistence of some dispersed particles and aggregates. When the concentration of PP increases continuously, there is an onset of interpenetrating co-continuous morphology, which is obtained at 50-60 wt.% PP concentration (Fig. 3(e),(f)). The PP phase and the EOC phase are completely continuous at this particular concentration region. Then there is a phase transformation. But the end of interpenetrating co-continuous morphology occurs at 30 wt.% EOC concentration(Fig 3(g)). This asymmetrical phenomenon is resulted from the fact that PP and EOC have different

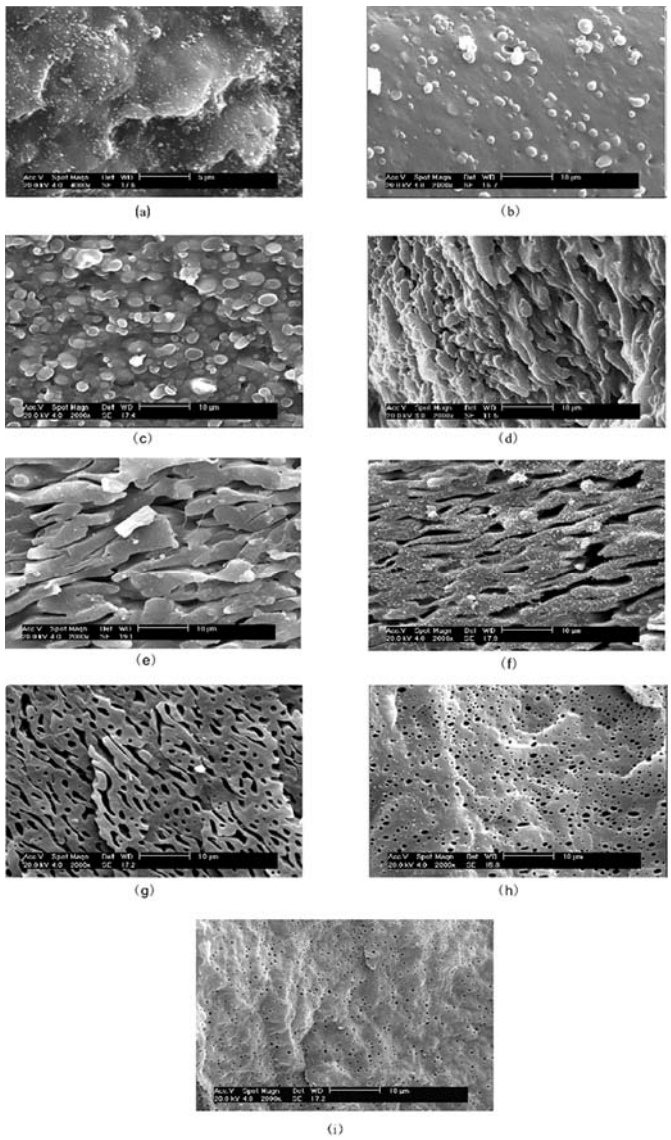

Fig. 3. SEM photomicrographs showing the effect of blend composition on the morphology development of PP/EOC blends (a)PP/EOC=10/90, (b)PP/EOC=20/80, (c)PP/EOC=30/70, (d)PP/EOC=40/60, (e)PP/EOC=50/50, (f)PP/EOC=60/40, (g)PP/EOC=70/30, (h)PP/EOC=80/20, (i) PP/EOC=90/10.

viscosities. When the major component is PP, the EOC component forms dispersed particles in the PP matrix phase. It is evident from Fig. 3(h)-(i) that spherical inclusions in plastic phase formed in the blends with lower EOC concentration, and spherical inclusions are obtained by removing the rubber phase using heptane. The average diameter and droplet size distribution of 10 wt.%, 20 wt.% EOC concentration are given in Fig. 4 and Fig. 6, respectively.

The effect of concentration on phase coarsening

It can be seen from Figs. 4-6 that the dispersed phase domain size increases as the concentration of dispersed phase increases, and the size distribution of the dispersed phase domain broadens simultaneously, regardless of the type of dispersed phase. This can be attributed to the increase of dispersed phase coalescence with dispersed phase concentration.

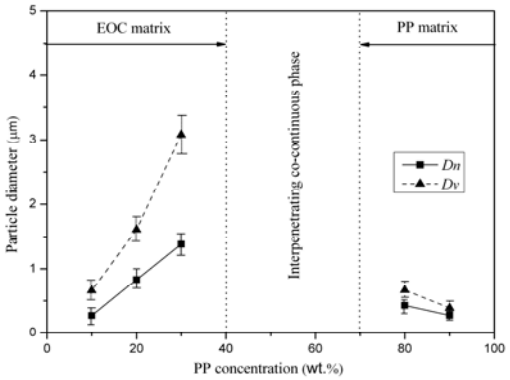

Fig. 4. The number average diameter (D_n) and the volume average diameter (D_v) of the dispersed phase as a function of the PP concentration. The error bars represent the deviations in the diameter measurements.

In the binary blends, drop breakup is not influenced by the volume fraction of the dispersed phase, while coalescence is strongly influenced [5]. As a result of mixing, drops of dispersed phase may tend to collide and coalesce eventually. That is, two drops become close to each other, the film of the matrix phase between the two drops drains, the film thickness decreases to a critical value, then rupture of the interface occurs, resulting in coalescence. Coalescence depends on two principal parameters: the number of droplet collision and the ability of the blends to drain the film of matrix phase entrapped between two droplets of the dispersed phase. The number of droplet collision is proportional to the square of the concentration of the dispersed phase, and is an inverse function of the particle size according to Smoluwchowski [41]:

$$N_{coll} = \frac{6C^2}{\pi^2 R^3} \qquad (4)$$

Where C is the disperse concentration, R is the droplet radius and N_{coll} is the number of droplet collision per unit volume and time. Film drainage is a complex phenomenon that depends directly on the interfacial tension between two fluids, and is in inverse proportion to the viscosity of the matrix [4]. But the aforementioned discussion is essentially based on studies considering the coalescence of two droplets with a controlled diameter only. When coalescence is studied in polymer blends, the phenomenon is complicated by high viscosity and elasticity of polymer. In addition, for concentrated blends, not only two but three or more droplets can meet and coalesce at the same time [5].

When the concentration of dispersed phase increases, the number of droplet collision increases. Besides, the interfacial tension between PP and EOC (Engage 8150) is very

small [38], and the smaller interfacial tension is, the more probable coalescence is. So the coalescence process in the PP/EOC blends increases as the concentration of dispersed phase increases. That leads to the increase of dispersed phase domain size.
A prominent feature in Fig. 5 and 6 is that the droplet size distribution broadens at higher dispersed phase concentrations. Breakup and coalescence occurred simultaneously during the mixing at the higher concentrations, which led to a much broader distribution of particle size. Very small particles may result from breakup in the high shear regions, while increased coalescence due to more drop interactions will result in very large particles.

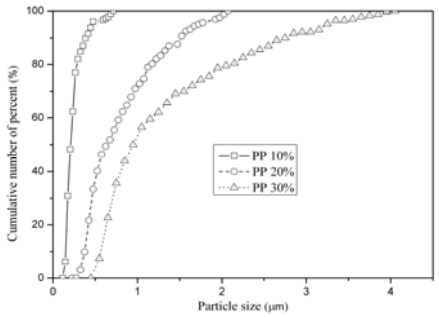

Fig. 5. The effect of PP concentration on the droplet size distribution in PP/EOC blends.

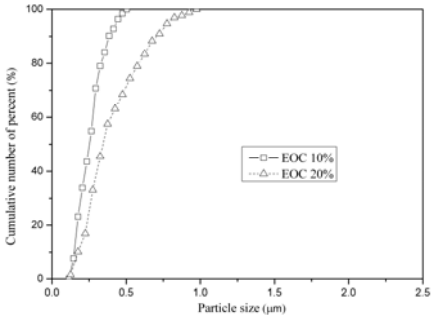

Fig. 6. The effect of EOC concentration on the droplet size distribution in PP/EOC blends.

Phase coarsening and phase fine dispersing

Comparing the photomicrographs of PP/EOC=80/20 with PP/EOC=20/80 in Fig. 3, different droplet sizes and size distribution are found, and the blends of 80 wt.% EOC concentration show a bigger drop size than the blends of 80 wt.% PP concentration. A similar phenomenon has been reported in the PS/PB blends [3]. The asymmetric phenomenon can be explained by the lower melt viscosity and storage modulus of the EOC phase compared to PP phase.
When the EOC phase becomes the matrix phase, $\eta_d > \eta_m$, the dispersed phase droplets deform hard in the shear field, the equilibrium between droplet breakup and coalescence shifts more in the direction of coalescence in mixing process. It is difficult to disperse the PP phase of a high melt viscosity into the EOC phase of a lower melt viscosity. So the coarse dispersed phase formed in the blends. Vice versa, when the PP phase becomes the matrix phase, $\eta_m > \eta_d$, based on the study of van Gisbergen [21], coalescence during mixing may also be governed by the interfacial mobility. The high viscosity of polymer matrix should give rise to a relatively immobile interface which should result in long drainage times for the intervening film, and the equilibrium between droplet breakup and coalescence shifts more in the direction of breakup in mixing process. Thus it is easy to disperse the EOC phase of a lower melt viscosity into the PP phase of a higher melt viscosity, and the fine-dispersed phase formed in the blends.
In addition, within the range of mixing and processing conditions, the shape of droplets is determined not only by the dissipative (viscous) force, but also by the pressure distribution around the droplet arising from the elasticity. VanOene H [30]

found that the drop elasticity has a stabilizing effect, which restrains drop deformation; higher elasticity of the dispersed than continuous phase result in more stable drops. The elasticity ratio of EOC to PP is 0.76 at 40 rpm (As shown in Table 2). When the dispersed phase is PP component, it shows higher elasticity than the continuous phase, resulting in a more stable drop. So the coarse dispersed phase formed in the PP/EOC (80/20) blends. Vice versa, the fine-dispersed phase formed in the PP/EOC (20/80) blends.

The effect of mixing time on the phase morphology development

The effect of mixing time on the phase morphology development in melting blend has been extensively studied [1,10,13-17]. The phase morphology development photomicrographs of PP/EOC (80/20) blends mixed at different mixing time are shown in Fig. 7. PP/EOC (80/20) blends was chosen to study the effect of processing

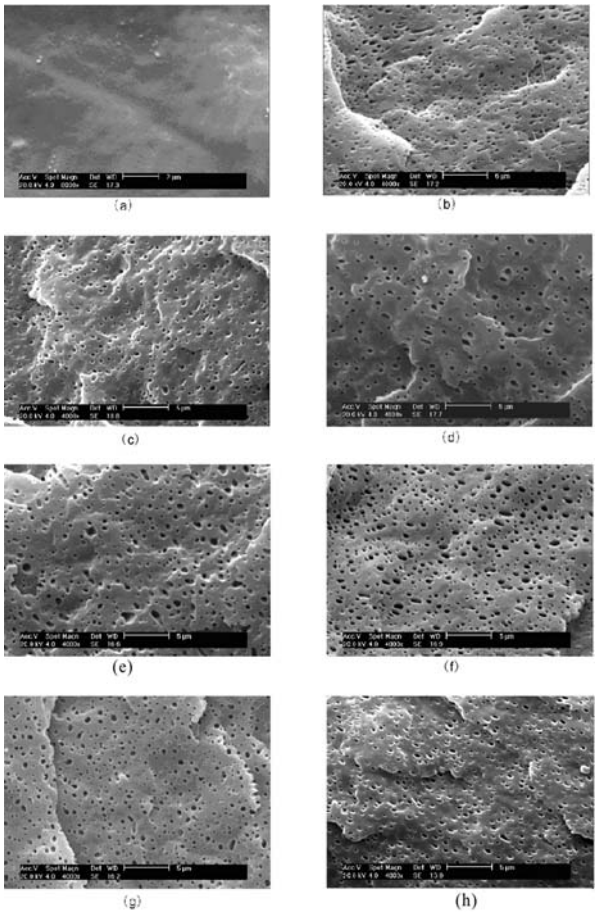

Fig. 7. SEM micrographs showing the morphology evolution of PP/EOC (80/20) blends as a function of mixing time: (a) 1 min, (b) 1.5 min, (c) 2 min, (d) 3 min, (e) 4 min, (f) 5 min, (g) 7 min, (h) 11 min.

conditions on phase morphology development of PP/POE blends. Since the brittle-ductile transition of the blends begins to occur in PP/EOC (80/20) [36]. Meanwhile, the phase morphology shows well-defined droplet-matrix morphology in this blend composition. In Fig. 7 (a)-(b), it can be observed that after 1.5 min of mixing time, PP/EOC (80/20) blends has already formed a well-established droplet/matrix morphology in which the PP component formed the matrix phase and the EOC component became the droplets dispersed in the matrix phase. From Fig. 7 (c) to Fig. 7 (h), the similar phase morphology persisted in the blends when the mixing time was extended to 11 min.

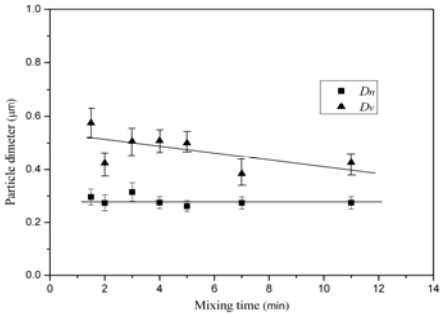

Fig. 8. The D_n and D_v of the dispersed phase as a function of the mixing time in PP/EOC (80/20) blends.

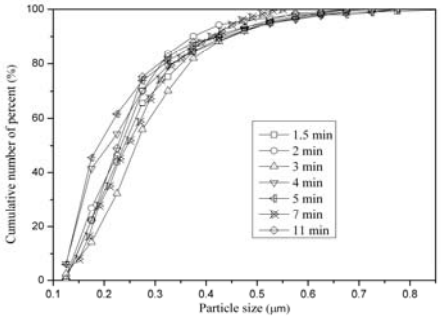

Fig. 9. The effect of mixing time on the droplet size distribution in PP/EOC (80/20) blends.

The number average diameter (D_n) and the volume average diameter (D_v) of the EOC domain as a function of the mixing time in PP/EOC (80/20) blends are presented in Fig. 8. The most significant domain break-up phenomenon occurred within the first 1-2 min of mixing, when melting and softening occurred. Based on the 'sheeting' mechanism [14], a large mass of the dispersed phase form the sheets or ribbons of the dispersed phase in the matrix at the melting and softening stage, then holes develop in the ribbons with the mixing time increasing, which grow in size and concentration until a fragile lace structure forms. The lace structure ultimately breaks up into spherical particles. But the EOC component did not form 'sheet' or 'thread' structures in shear flow due to the low melting temperature of the EOC component and the long mixing time calculated in our study. The phase dimensions did not change significantly with further increase of mixing time. The invariant morphology was dependent on the dynamic equilibrium between droplet breakup and coalescence.
Fig. 9 shows that the size distribution of dispersed phase domain remains unchanged when the mixing time increases. During mixing, the dispersed phase broke down until a minimum droplet size was reached; the drop breakup became more and more difficult, while coalescence was occurring simultaneously during mixing process, attaining a dynamic equilibrium between breakup and coalescence for a short time. So the size distribution of dispersed phase domain kept constant.

The effect of rotor speed on the phase morphology development of PP/EOC blends

Taylor [18,19] studied the deformation of a single Newtonian drop in steady shear flow. He modeled the deformation of a drop by two dimensionless parameters:

$$\lambda = \frac{\eta_d}{\eta_m} \tag{5}$$

$$Ca = \frac{\eta_m \gamma}{\tau / d} \tag{6}$$

Where η_d and η_{rn} are the viscosity of dispersed and continuous phases, γ and τ are shear rate, interfacial tension, and d is droplet diameter, λ and Ca are viscosity ratio and capillary number, respectively.

The numerator of Eq. (6) is the shear stress ($\sigma = \eta_{rn} * \gamma$) imposed on the continuous phase by screw rotation. The denominator of Eq. (6) is the interfacial stress which acts as the resistance against deformation, and deformation occurs only for Ca greater than the critical value.

But molten polymers are viscoelastic liquid in the mixing process, the deformation of drop is determined not only by the dissipative forces, which is characterized by the numerator of Eq. (6), but also by the pressure distribution around the droplet from the elasticity. Therefore, Taylor's equation is not valid to characterize the drop deformation and breakup in viscoelastic systems [20,22].

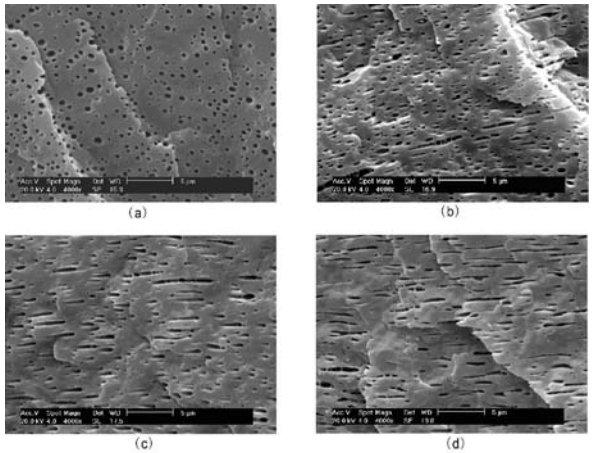

Fig. 10. SEM micrographs showing the morphology evolution of PP/EOC (80/20) blends as a function of rotor speed: (a) 32 rpm, (b) 50 rpm, (c) 60 rpm, (d) 70 rpm.

The phase morphology development photomicrographs of PP/EOC (80/20) blends mixed at different rotor speeds are given in Fig. 10. Fig. 3 (h) represents the photomicrograph at a rotor speed of 40 rpm. The mixing was performed in an internal mixer for 10 min at 180°C. The number average diameter (D_n) increased slightly, while the volume average diameter (D_v) of the dispersed phase increased, and the size distribution of the dispersed phase domain broadened simultaneously as the rotor speed increased (see Table 2).

It is obvious that Taylor theory can not explain the above experiment results, which may be attributed to the drop coalescence resulted from the increase of shear rate. In Table 2, one can see that the viscosity ratio remains approximately invariable over a shear rate range of 50-110 s^{-1}. But both the elasticity and elasticity ratio increase as

the shear rate increases in Fig. 2 and Table 2. VanOene H [30] reported that the drop elasticity has a stabilizing effect, which restrains drop from breaking. Therefore, the increasing of elasticity and elasticity ratio may prevent the drop from occurring breakup and lead to higher degree coalescence. The dispersed phase domain size increases, and the size distribution of dispersed phase domain broadens simultaneously as the shear rate increases.

The most prominent phenomenon in Fig. 10 is the variation of dispersed phase domain shape with the rotor speed. The dispersed phase domain deforms from spherical droplet to elliptical droplet, even fibrillar or sheet morphology. The influence of rotor speed on the shape factor of the dispersed phase droplets is given in Table 2. The deformation extent of drop can be characterized by the shape factor, which is defined by the length (major axis of ellipse) to width (minor axis of ellipse) ratio of the dispersed particles. The dispersed phase domain is considered as spherical or near spherical when the shape factor is 1-1.5 for samples. When the value of shape factor increases further, the elliptoid, even fibrillar or sheet morphology will appear.

Table 2. The various parameters of different rotor speed in the PP/EOC (80/20) blends

Rotor speed(rpm)	Shear rate(s^{-1})	Viscosity ratio[a]	Elasticity ratio[b]	D_n (μm)	D_v (μm)	Size distribution[c]	Shape factor
32	51.2	0.27	0.68	0.33	0.46	1.39	1.50
40	64	0.26	0.76	0.42	0.66	1.57	1.45
50	80	0.27	0.83	0.34	0.64	1.88	2.82
60	96	0.27	0.94	0.40	0.80	2.00	3.32
70	112	0.28	-----	Sheet	Sheet	----	4.45

a Viscosity ratio based on the ratio between η_{EOC} and η_{PP}.
b Elasticity ratio based on the ratio between G'_{EOC} and G'_{PP}.
c Size distribution based on the ratio between D_v and D_n.

Drop-to-fibril transition in Newtonian fluids was previously studied by some investigators [23]. They pointed out that if the viscosity ratio was close to unity, a uniform thin-thread fibrillar morphology formed. However, in viscoelastic fluids, fibrillar morphology was reported at $0.3<\lambda<1.0$ for PE/PS blends [24], $\lambda<1.0$ for PP/EPR blends [25]. In our system, the interfacial tension remains invariable, and the viscosity ratio remains approximately invariable ($\lambda\approx0.27$), and the elasticity ratio increases as the shear rate increases. Therefore, the drop-to-fibril transition is dependent on the increase of shear rate and elasticity ratio.

Conclusion

The effects of blend composition and processing conditions on phase morphology development of PP/EOC blends were investigated. It is obvious from SEM photomicrographs that the minor composition formed the dispersed phase and the major composition formed the continuous phase, and at the intermediate concentration the blends formed interpenetrating co-continuous morphology. The increase of dispersed phase coalescence with dispersed phase concentration was applied to interpret the effect of concentration on phase coarsening. The asymmetric phenomenon in PP/EOC (80/20) blends and PP/EOC (20/80) blends can be explained by different melt viscosity and storage modulus. The PP/EOC (80/20) blends formed

a well-established droplet/matrix morphology after 1.5 min of mixing. The similar phase morphology persisted in the blends when the mixing time was extended to 11 min. The most prominent phenomenon is that the dispersed phase domain deformed from spherical droplet to elliptical droplet, even fibrillar or sheet morphology as the rotor speed increased. The increase of shear rate and elasticity ratio was applied to interpret this phenomenon.

Acknowledgements. The authors gratefully acknowledge the financial support of National Natural Science Foundation of China (No. 02490220).

References

1. Nair SV, Oommen Z, Thomas S (2002) J Appl Polym Sci 86:3537
2. Jose S, Nair SV, Thomas S, Karger-Kocsis J (2006) J Appl Polym Sci 99:2640
3. Jose S, Thomas S (2003) Eur Polym J 39:115
4. Elmendorp JJ, Van Der Vegt AK (1986) Polym Eng Sci 26:1332
5. Sundararajs U, Macosko CW (1995) Macromolecules 28:2647
6. Zeng JJ, Aoyama M, Takahashi H (2003) J Appl Polym Sci 89:1791
7. Jaziri M, Kallel TK, Mbarek S (2005) Polym Int 54:1384
8. Paul DR, Barlow JW (1980) J Macromol.Sci Rev Macromol Chem 18:109
9. Bhadane PA, Champagne MF,Huneault MA,Tofan F, Favis BD (2006) Polymer 47:2760
10. Thomas S, Groeninckx G (1999). J Appl Polym Sci 71:1405
11. Asadinezhad A, Yavarıı A, Jafari SH, Khonakdar HA, Hässler R (2005) Polymer Bull 54:05
12. Chaudhry BI, Hage E, Pessan LA (1998) J Appl Polym Sci 67:1605
13. Scott CS, Macosko CW (1995) Polymer 36:461
14. Sundararaj U, Macosko CW, Shih CK (1996) Polym Eng Sci 36:1769
15. Scott CS, Macosko CW, Rolando RJ, Chan HT (1992) Polym Eng Sci 32:1814
16. Willemse RC, Ramaker EJJ, van Dam J, Posthuma de Boer A (1992) Polymer 40:6651
17. Favis BD (1992) J Appl Polym Sci 39:285
18. Taylor GI (1932) Proc R Soc Lond A 138:41
19. Taylor GI (1934) Proc R Soc Lond A 146:501
20. Grizzuti N, Bifulco O (1997) Rheol Acta 36:406
21. Van Gisbergen(1991) J. Ph. D. Thesis Eindhoven University of Tevhnology, Eindhoven, The Netherlands
22. Roland CM, Bohm GGA (1984) Polym Sci., Polym. Phys 22:79
23. Tomotika S, Cox R., Mason SG (1972) J Colloid Sci 38:395
24. Min K, White JL, Fellers JF (1984) Polym Eng Sci 24:1327
25. Kim BK, DO IH (1996) J Appl Polym Sci 60:2207
26. Zhang L, Huang R, Li LG, Wang G (2002) J Appl Polym Sci 83:1870
27. Lee JK, Han CD(1999) Polymer 40:6277
28. Wu S (1987) Polym Eng Sci 27:335
29. Favis BD, Chalifoux JP (1987). Polym Eng Sci 27:1591
30. VanOene H (1972) J Colloid Interface Sci 40:448
31. Da Silva ALN, Rocha MCG, Coutinho FMB, Bretas R, Scuracchio C (1997) J Appl Polym Sci 66:2005
32. Da Silva ALN, Rocha MCG, Coutinho FMB, Bretas R, Scuracchio C (2002) J Appl Polym Sci 75:692
33. Da Silva ALN, Rocha MCG, Coutinho FMB, Bretas RES, Farah M (2002) Polymer Testing 21:647
34. Paul S, Kale DD (2002) J Appl Polym Sci 84:665
35. Paul S, Kale DD (2000) J Appl Polym Sci 76:1480

36. Yang J, Zhang Y, Zhang Y (2003) Polymer 44:5047
37. McNally T, McShane P, Nally GM, Murphy WR, Cook M, Miller A (2002) Polymer 43:3785
38. Kontopoulou M, Wang W, Gopakumar TG, Cheung C (2003) Polymer 44:7495
39. Carriere CJ, Silvis HC (1997) J Appl Polym Sci 66:1175
40. Li Jiashen (2001) Ph. D. Thesis, Tianjin University, Tianjin, China
41. Smoluwchowski M (1917) Z Physik Chem 92:129